Canadian Journal of Forest Research

Research Article

Long-term declines in nitrogen and other nutrients in foliage of three northern hardwood species at the Hubbard Brook Experimental Forest

Nina K. Lany[a], **Linda H. Pardo**[b], **Natalie L. Cleavitt**[c], **Timothy J. Fahey**[c], **and Christine L. Goodale**[d]

[a]USDA Forest Service, Northern Research Station, North Woodstock, NH 03262, USA; [b]USDA Forest Service, Northern Research Station, Burlington, VT 05405, USA; [c]Department of Natural Resources and the Environment, Fernow Hall, Cornell University, Ithaca, NY 14853, USA; [d]Department of Ecology and Evolutionary Biology, Corson Hall, Cornell University, Ithaca, NY 14853, USA

Corresponding author: **Nina K. Lany** (email: nina.lany@usda.gov)

Abstract

Forests of the northeastern US have experienced multiple environmental changes over the last three decades, including rising temperatures and atmospheric CO_2 concentrations and declines in acidic deposition, including nitrogen (N) deposition. We used measurements over a 32-year time span (1992–2023) from the Hubbard Brook Experimental Forest, New Hampshire, USA to assess the overall impact of these environmental changes on foliar chemistry (N, carbon, and phosphorus concentrations) and isotopic composition (δ^{15}N and δ^{13}C) of three dominant northern hardwood species: sugar maple, American beech, and yellow birch. Intrinsic water use efficiency estimated from foliar δ^{13}C increased for all three species in response to rising atmospheric CO_2 concentrations. Foliar N concentrations showed large declines after peaks during 2001–2006. These responses are likely driven by the combination of rising atmospheric CO_2 and declining N deposition, but we cannot distinguish between these drivers. Foliar δ^{15}N and N:P ratios declined over the study period for sugar maple but not for American beech and birch. Foliar C concentrations declined for all three species, but larger relative declines in foliar N than C led to increases in foliar C:N ratios, which could further slow N mineralization rates and amplify N limitation in forests where these impacts are present.

Key words: foliar nitrogen, Hubbard Brook Experimental Forest, δ^{15}N, δ^{13}C, intrinsic water use efficiency

Introduction

In forests, foliar nitrogen (N) sits at the nexus of photosynthesis and energy capture from the sun, thereby impacting primary productivity, N cycling rates in the soil, and ecosystem capacity for carbon accumulation. Foliar N and photosynthesis, in turn, affect carbon allocation, light interception, tissue chemistry, and a variety of related plant traits (Reich et al. 1997), and can drive changes in soil N availability that affect soil respiration (Bae et al. 2015). Furthermore, foliar N is fundamentally important to herbivore nutrition (Mattson 1980) and affects the trophic structure of ecosystems (Cebrian et al. 2009). However, foliar N concentration is responsive to shifts in atmospheric carbon dioxide (CO_2) concentration and N availability (Xu et al. 2020; Gojon et al. 2023). Elevated atmospheric CO_2 concentrations usually induce decreases in the concentrations of N and some other nutrients in plant tissues (Cotrufo et al. 1998; Reich et al. 2006; Penuelas et al. 2020; Gojon et al. 2023), but do not lead to consistent changes in foliar carbon (C) or phosphorus (P) concentrations, and thus generally result in overall increases in C:N and decreases in N:P ratios (Xu et al. 2020). Warmer air temperatures also reduce foliar N, as plants compensate for increased metabolic efficiency at warmer temperatures by decreasing foliar N and P concentrations (Haxeltine and Prentice 1996). Foliar nutrient concentrations also respond to changes in N availability resulting from altered N inputs. Foliar N typically increases in N addition experiments; foliar concentrations of C, P, calcium (Ca), and other nutrients can also respond (Gundersen et al. 1998; Högberg et al. 2006; Xu et al. 2020). Foliar N also regularly increases across gradients of N deposition, such as that in the northeastern US (Crowley et al. 2012). Correspondingly, we expect reductions in N deposition to lead to declines in foliar N. These leaf-level nutrient declines may be exacerbated by feedbacks that increase N limitation through the accumulations of nutrients in biomass, immobilization in detritus, and slowing of nutrient mineralization rates (Luo et al. 2004).

Stable isotope ratios of nitrogen (δ^{15}N) and carbon (δ^{13}C) in plant tissue can be used as integrative measures of ecosystem N and C cycles. Lower foliar δ^{15}N values can indicate tighter N cycling and less N loss (Högberg 1998). Foliar δ^{15}N has been used as an indicator of soil N availability to plants and the openness of the N cycle, and the N-saturation status of forest ecosystems (Pardo et al. 2006; Norby et al. 2010; Sabo et

al. 2020). When combined, data on $\delta^{13}C$ and $\delta^{15}N$ can indicate the ways the C and N cycles interact under increasing atmospheric CO_2 and altered N inputs (e.g., Guerrieri et al. 2011). Both increasing CO_2 and declining N deposition should decrease foliar $\delta^{15}N$ as N becomes more limiting to plants. Stable isotope ratios of carbon ($\delta^{13}C$) of plant tissue are used to calculate intrinsic water use efficiency (iWUE), the ratio of photosynthesis to stomatal conductance (Farquhar et al. 1982); higher iWUE is correlated with higher (less negative) $\delta^{13}C$. iWUE inferred from $\delta^{13}C$ of tree rings has increased over time across the world along with rising atmospheric CO_2 (Peñuelas et al. 2011; Silva and Anand 2013). iWUE can also increase in response to N additions (Guerrieri et al. 2011) because added N can stimulate photosynthesis more than it increases stomatal conductance. Thus, rising atmospheric CO_2 and decreasing N deposition should exert opposing effects on iWUE, even as both processes are likely to drive declines in foliar N concentration.

At the Hubbard Brook Experimental Forest (HBEF) in New Hampshire, USA, foliar chemistry has been measured along an elevation gradient for more than three decades, providing an opportunity to assess how forests of the northeastern US are responding to net effects of changes in multiple environmental drivers. Previous studies along the elevation gradient at the HBEF have demonstrated increased soil N availability, foliar N, and litter N with increasing elevation within the northern hardwood forest zone (Bohlen et al. 2001; Fahey et al. 2025*a*).

In the present study, we analyzed a 32-year time series (1992–2023) of foliar chemistry measurements of three co-dominant hardwood tree species: sugar maple (*Acer saccharum* Marsh.), American beech (*Fagus grandifolia*, Ehrh.), and yellow birch (*Betula alleghaniensis* Britt.). Over this time period, atmospheric CO_2 has increased by 19% (68 ppm) globally (Keeling et al. 2005), while mean annual air temperature at the HBEF has increased by approximately 2.1 °C (USDA Forest Service, Northern Research Station 2025) and annual precipitation is 242 mm greater, a 17% increase (USDA Forest Service, Northern Research Station 2024). Anthropogenic activities greatly increased rates of N deposition across the eastern US during the latter half of the 20th century. However, rates of N deposition have declined steeply during the 21st century due largely to reductions in N emissions in response to the Clean Air Act and 1990 Amendments (Driscoll et al. 2024). Bulk deposition of N and sulfur (S) at Hubbard Brook have decreased by ~44% (-5.4 kg N ha^{-1} $year^{-1}$) and ~80% (-8.9 kg S ha^{-1} $year^{-1}$) during the period of study (Hubbard Brook Watershed Ecosystem Record (HBWatER), 2024). We hypothesized that:

1) foliar N concentrations, $\delta^{15}N$, and N:P ratios would decline and C:N ratios increase over time for all three co-dominant species, consistent with expectations of increased N limitation from both decreasing N deposition and rising atmospheric CO_2; and
2) $\delta^{13}C$-based iWUE would increase over time in response to rising atmospheric CO_2, although increasing N-limitation could suppress this response.

Methods

Site description

The HBEF is located in the White Mountain National Forest in central New Hampshire, USA (43°56′N, 71°45′W). Foliage sampling occurred at four northern hardwood forest plots west of Watershed 6 (the biogeochemistry reference watershed at the HBEF), in mature forest stands that have been unmanaged since heavy cutting in the early 20th century (Fahey et al. 2022). The 1.25 ha plots are arranged along a 240 m elevation gradient: 550 m a.s.l. (Low), 625 m a.s.l. (Mid), 725 m a.s.l. (Upper), and 790 m a.s.l. (High). Plots are each separated by approximately 500–600 m ground distance. Measurements of soil N cycling (Bohlen et al. 2001) and long-term leaf litterfall (Fahey et al. 2022) in these plots have been reported previously. The climate is humid continental, with ~1400 mm of annual precipitation evenly distributed across the year on average (USDA Forest Service, Northern Research Station 2024), and monthly mean temperatures (1956–2023) of −8 °C in January and 19 °C in July (USDA Forest Service, Northern Research Station 2025). On average, annual precipitation was 77 mm greater and mean air temperature decreased by approximately 1.5 °C from low- to high-elevation plots along this gradient. Bulk atmospheric N deposition averaged 5.3 kg N ha^{-1} $year^{-1}$ over the study period (Hubbard Brook Watershed Ecosystem Record (HBWatER), 2024). The vegetation, typical of northern hardwood forests, is composed primarily of American beech, sugar maple, and yellow birch, with red spruce (*Picea rubens* Sarg.) and balsam fir (*Abies balsamea* (L.) Mill.) increasing at the highest elevations (van Doorn et al. 2011). Soils are primarily acidic Spodosols derived from glacial till with organic surface horizons that average ~6 cm in the hardwoods and ~9 cm in spruce–fir (Johnson et al. 2000) over bedrock of schist and granulite (Bailey et al. 2019).

Foliage sampling and chemical analysis

Beginning in 1992, foliage samples were collected from co-dominant sugar maple, American beech, and yellow birch trees annually in August, but were collected in late July in 2017, 2019, 2022, and 2023. From 1992 to 2017, canopy leaves were obtained by climbing one individual of each focal canopy species at each plot and clipping a sun-exposed branch. The same trees were sampled each year, except that the beech individual at the High plot was replaced in 2008 after a period of declining health (2005–2007). Foliage was not collected in 2009, 2012, 2014, and 2016. Beginning in 2018, samples were obtained via shotgun sampling from three individuals of each species within each plot. The same individuals were not sampled across years to minimize the impact of sampling on the trees. For both sampling approaches, foliage samples were obtained from mid-to-upper canopy branches and consisted of approximately 30 pooled sun leaves, but the number of leaves per sample ranged from 15 to 100.

Following collection, any attached woody material was removed prior to drying leaf samples for 48 h at 60 °C, until thoroughly dry. Nitrile gloves were worn while handling leaf material. Samples were finely ground and were dried again in jars with caps loosened at 60 °C for 24 h before chemi-

cal analysis. Samples were analyzed for C and N content at the USDA Forest Service Forest Sciences Laboratory (Durham, New Hampshire, USA) with a Thermo Flash EA 1112, except for 2010 and 2011 when they were analyzed with an Elementar vario EL at Cornell University (Ithaca, New York, USA). Samples were typically analyzed within a year of collection from 2013 to 2023, and samples collected during 1992–2009 were reanalyzed at the USDA Forest Service Forest Sciences Laboratory in 2024. Samples from 2013 and 2015 were analyzed at the Durham lab both at the time of collection and in 2024 for comparison. No significant difference was found between the N concentrations measured in the original analyses and the 2024 re-analysis across the three canopy species combined (paired t test: $t = -1.36$, df $= 22$, $p = 0.19$, Fig. S1). Foliar C concentrations measured in the 2024 re-analysis were 0.6 ± 0.3%C higher than the original analysis (paired t test: $t = -4.09$, df $= 22$, $p < 0.01$, Fig. S2).

Isotopic analyses were performed at the Center for Stable Isotope Biogeochemistry at University of California, Berkeley with a Finnigan MAT DeltaPlus XL isotope ratio mass spectrometer in continuous flow (Thermo Scientific, Bremen, Germany). δ^{15}N values represent the per mil difference between the isotopic composition of the sample and that of atmospheric dinitrogen. δ^{13}C values represent the per mil difference between the sample and Vienna Pee Dee Belemnite reference. Samples from 2001–2023 were typically analyzed within a year of collection, and samples collected during 1993–2000 were analyzed in 2024.

For measurements of foliar P concentrations, samples were analyzed at Yale University from 1992 to 2003 using the ashed crucible method (Johnson et al. 2014). A 0.3 g sample of the oven-dry ground material was ashed and dissolved in nitric acid and determined for each sample using a Perkin Elmer Optima 3000 ICP spectrometer. Samples from 2004 to 2008 were analyzed using microwave digest (EPA method 3052) and a Perkin Elmer PE-3300DV ICP Spectrometer at the University of Michigan. Samples from 2012 to 2022 were analyzed using microwave digest and an Agilent 730 ICP-OES at the USDA Forest Service Forest Sciences Laboratory. Beginning in December 2022, samples were analyzed on the newly installed Agilent 5900 ICP-OES at the USDA Forest Service lab. Samples from 2010 and 2011 were not analyzed for P concentration.

All chemistry measurements for the American beech tree at the High elevation plot were removed for leaves gathered in 2005, 2006, and 2007 due to rapidly declining tree health. Data were also removed for the American beech at the Upper elevation plot in 1997 due to improbably low measured concentrations for many elements. Data are published at the Environmental Data Initiative (Fahey et al. 2025*b*).

iWUE calculation

iWUE (μmol/mol) was calculated from measurements of δ^{13}C in foliage ($\delta^{13}C_p$) according to eq. 1:

$$\text{(1)} \qquad \text{iWUE} = \frac{C_a}{1.6} \times \frac{b - \delta^{13}C_a + \delta^{13}C_p}{b - a}$$

where a is the ^{13}C fractionation of diffusion of CO_2 ($a = 4.4$ ‰), b is the ^{13}C fractionation by Rubisco ($b = 27$ ‰), C_a is the CO_2 concentration of the atmosphere during August of each year, and $\delta^{13}C_a$ is the atmospheric stable carbon isotope concentration in August of each year (Farquhar et al. 1989; Guerrieri et al. 2011, 2016). Monthly C_a and $\delta^{13}C_a$ concentrations were obtained from the Mauna Loa Observatory (Keeling et al. 2005). The August $\delta^{13}C_a$ was not available for 2023, so a value was estimated through linear extrapolation of $\delta^{13}C_a$ over time.

Other variables

Additional data on possible variables explaining variation in foliar N were gathered at the HBEF, and included soil potential N mineralization, mean air temperature over June and July, and bulk N deposition. Soil potential N mineralization rates (mg N kg_{soil}^{-1} day^{-1}) were measured on three of the four plots in this study (Low, Mid, and High elevation, but not Upper) from 1994 to 2023 (Groffman and Martel 2025). Five soil cores were collected to a depth of 10–15 cm from each plot in July each year and separated into three groups (combined Oi/Oe, combined Oa/A, and upper mineral soil). Potential net N mineralization rates were quantified for each group as the difference between an initial 2 mol/L KCl extraction and the accumulation of inorganic N (NH_4^+ plus NO_3^-) during a 10-day laboratory incubation at field moisture. Data from the Oa/A horizon sample in each of the five cores per plot were averaged for analysis. Daily maximum and minimum air temperatures (°C) were recorded at weather station 1, located near the Low elevation plot at 478 m elevation (USDA Forest Service, Northern Research Station 2025). Daily maximum and minimum temperatures were averaged to obtain daily mean temperatures, which were then averaged over June and July to represent the growing season temperature prior to foliage sampling. Bulk inorganic N deposition was calculated using the method traditionally used at the Hubbard Brook Experimental Forest (Buso et al. 2000). That is, daily watershed precipitation volume (mm ha^{-1} day^{-1}) was multiplied by the corresponding solute concentration (mg/L) of the sample collected at the end of each weekly sampling interval (Hubbard Brook Watershed Ecosystem Record (HBWatER) 2024). One flux value per solute representing all of watershed 6 (i.e., for all four elevations) was summed for the year between 1 June and 31 May (water-year). Total inorganic N deposition (kg N ha^{-1} $year^{-1}$) was calculated from contributions of N from ammonium (NH_4^+) and nitrate (NO_3^-) ions. Field and laboratory methods are described in detail within each published data package.

Statistical methods

We tested for trends over time in each elemental foliar concentration (N, C, and P, as % or ppm), C:N and N:P ratios, as well as δ^{15}N, δ^{13}C, and iWUE for each of the three tree species with linear mixed-effects models. Models containing year as continuous predictor and plot as a random intercept were fit using the *lme* function in the R package *nlme* (Pinhiero et al. 2025; R Core Team 2025). Models were fit for each tree species separately, and random slope models were not considered. A within-plot temporal AR1 correlation structure (i.e., a 1-

year lag) was included in all models because foliar chemistry time series are expected to exhibit high temporal autocorrelation due to nutrient resorption (Aerts 1996). For 2018–2023, data from the three individual trees per species at each elevation were averaged prior to statistical analyses. We also fit quadratic models that included both year and year^2 as predictors because we thought foliar nutrients could increase as the ecosystem approaches N-saturation and then decrease, or they could decrease constantly over the record. The year^2 term was dropped from the model if the coefficient was not significant at $\alpha = 0.05$. Trends along the elevation gradient in each of the foliar chemistry variables (C, N, and P concentration, C:N and N:P ratio, δ^{15}N and δ^{13}C, and iWUE) were tested with linear mixed-effect models that contain elevation as a continuous numeric predictor and a random effect for year to account for dependence among samples collected within the same year.

Relationships between mean annual foliar N concentration and the hypothesized drivers of long-term trends were evaluated with linear regression and Akaike information criterion (AIC) model selection. (Burnham and Anderson 2004). Atmospheric CO_2 from Mauna Loa (ppm) during August, the 3-year running average of total bulk N deposition (kg N ha^{-1} year^{-1}), potential soil N mineralization rate (mg N kg$_{soil}^{-1}$ day^{-1}) in the previous July, and mean air temperature (°C) during June and July of the current growing season were each included as an explanatory variable in separate linear regressions. These hypothesized drivers were highly correlated over the study period (Fig. S3) and thus could not be included as covariates in the same model due to multicollinearity and cannot be meaningfully disentangled in this study. Foliar N concentration was averaged across all four plots within each year, and potential soil N mineralization rate was averaged across the three measured plots within each year. Choices about smoothing and time-lags were made based on the mechanism by which each variable would affect foliar N. In particular, CO_2 and air temperature directly affect photosynthesis, and thus foliar N, within the same growing season. In contrast, soil N availability during a growing season affects the nitrogen content of the developing leaf buds and thereby the foliar chemistry of leaves in the subsequent growing season. N deposition was averaged over a 3-year period to better capture its overall N input rather than its interannual variability. For each tree species, we compared models that included one of the hypothesized drivers of the average foliar N across all plots (one value per year) to each other and to an intercept-only model. A model was considered to have support if it was within $\Delta 2$ AIC$_c$ of the lowest AIC$_c$ model. We used AIC corrected for small sample size (AIC$_c$) because the sample size is small in this analysis of data that were averaged within each year ($n = 22$ years for all models). All statistical tests were performed in R 4.5.0 (R Core Team 2025).

Results

Nitrogen and δ^{15}N

Foliar N concentration increased during earlier years and then declined more recently for all three species (Fig. 1). Foliar N increased from 1993 until about 2001 for sugar maple, 2004 for American beech, and 2006 for yellow birch, followed by steep declines (Fig. 1; Table 1). Foliar N decreased from high to low elevation over the 240 m elevation gradient for both sugar maple and yellow birch but did not vary with elevation for American beech (Fig. 1; Table S1).

Foliar δ^{15}N declined linearly over time by 0.94 ‰ for sugar maple (Fig. 1; Table 1) but did not show any significant trends over time for either American beech or yellow birch (Fig. 1; Table 1). There were relatively large decreases in foliar δ^{15}N (1.22–1.44 ‰) from high to low elevation for all three species (Fig. 1; Table S1).

Foliar C and P concentrations and ratios with N

Foliar C and P concentrations both changed over time for all three tree species, but these changes were small relative to changes in N, such that temporal patterns in C:N and N:P ratios were driven by the larger relative changes in N concentrations rather than by patterns in C or P. Foliar C decreased over the measurement period for all three species (Fig. 2; Table 1). Foliar C:N ratios showed nonlinear (quadratic) patterns of first decreasing gradually and later increasing more steeply for all three species, driven by their relatively larger nonlinear declines in foliar N than C concentrations (Fig. 2; Table 1).

Foliar P concentrations declined linearly for American beech over the period of record. For both sugar maple and yellow birch, foliar P increased over the first half of the measurement period, and then decreased (Fig. 3; Table 1). Foliar N:P ratios decreased linearly over time for sugar maple, dominated by the steeper linear decline in foliar N than P (Figs. 2 and 3; Table 1). American beech foliar N:P increased in the middle part of the record but had no net change between the start and end of the record (Fig. 3; Table 1). No significant temporal patterns in foliar N:P were observed for yellow birch (Fig. 3; Table 1).

Foliar N drove spatial as well as temporal patterns in C:N and N:P ratios. Along the elevation gradient, foliar C increased from low to high elevation for sugar maple and beech, while yellow birch showed no significant elevational trend (Table S1). Foliar C:N of sugar maple and yellow birch showed small decreases with elevation, while American beech C:N had no trend with elevation (Table S1). No species showed significant elevational trends in P concentration and increases in N:P along the elevation gradient were observed for the two species (sugar maple and yellow birch) with elevational patterns in foliar N (Table S1).

δ^{13}C and iWUE

Foliar δ^{13}C declined in the early part of the record and increased slightly in recent years for both American beech and yellow birch (a positive quadratic relationship) but showed no trend for sugar maple (Table 1; Fig. 4). iWUE, which considers changes in atmospheric CO_2 and δ^{13}C as well as changes in foliar δ^{13}C (eq. 1), increased linearly over time for sugar maple and showed a positive quadratic pattern over time in American beech and yellow birch (Fig. 4; Table 1). Both δ^{13}C and iWUE decreased from high to low elevation for Ameri-

Fig. 1. Trends in foliar N concentration (left) and δ^{15}N (right) in co-dominant tree species at the Hubbard Brook Experimental Forest, 1992–2023. Solid lines indicate that coefficients were significant at $p < 0.05$. The line from the best fit model (linear vs. quadratic) is shown.

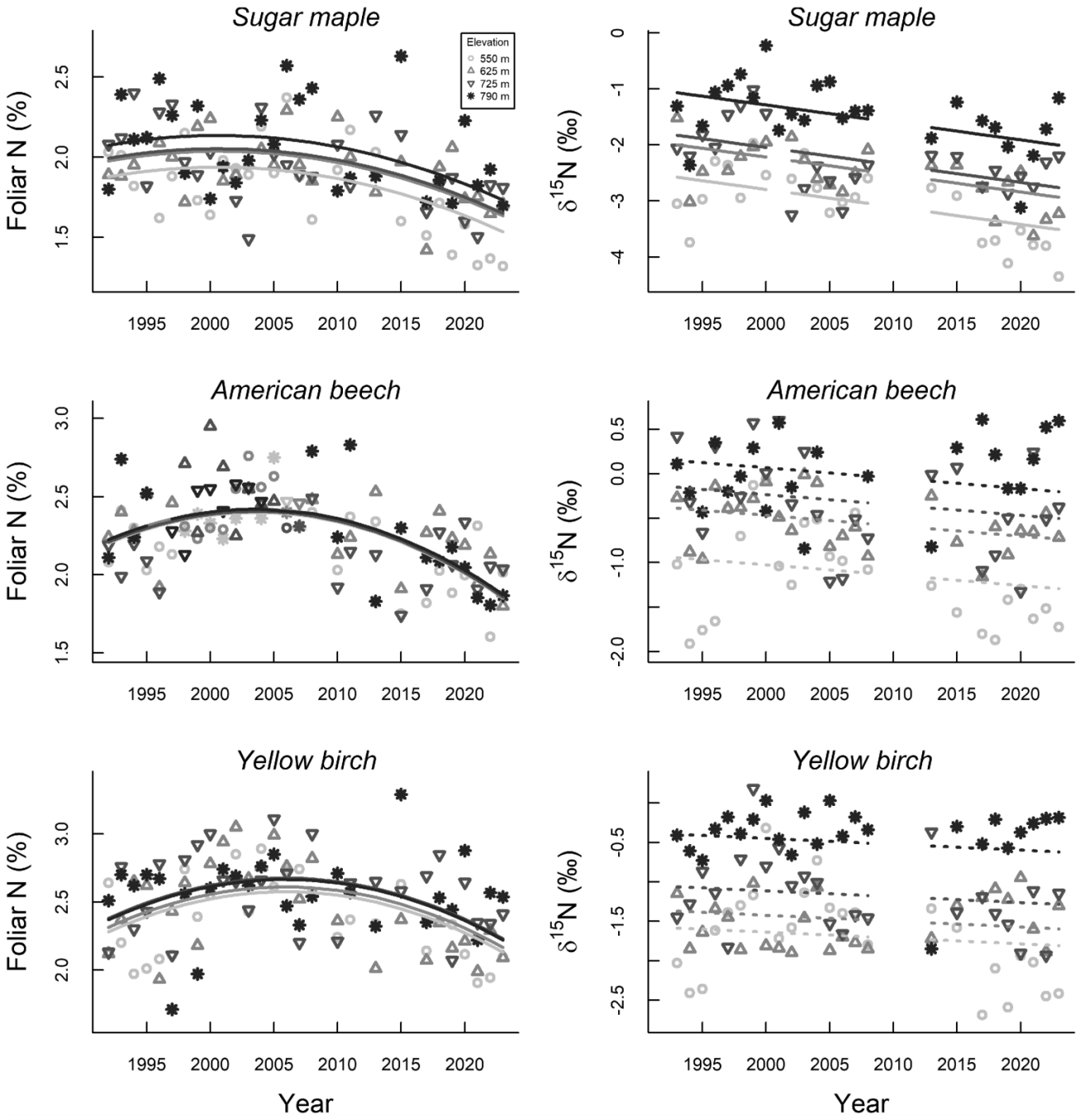

can beech and yellow birch, but did not differ by elevation for sugar maple (Table S1).

Relationships between foliar N and other variables

Atmospheric CO_2 (ppm) and mean air temperature during June and July (°C) increased, while bulk N deposition (kg N ha^{-1} $year^{-1}$) and July potential soil N mineralization (mg N kg_{soil}^{-1} day^{-1}) decreased over the period of study (Fig. S4). N deposition and atmospheric CO_2 were highly correlated ($r = -0.91$, Fig. S3), and correlations between potential soil N mineralization and both N deposition ($r = 0.60$) and atmospheric CO_2 ($r = -0.55$) were also strong (Fig. S3), highlighting that these variables cannot be meaningfully disentangled in this study. Best-fit models of annual foliar N concentration (averaged across all plots) for all three species included atmospheric CO_2 (Table 2; $n = 22$ years). For yellow birch, information criteria also indicated support for mean air temperature during June and July of the current growing season and the intercept-only model

Table 1. Trends over time in foliar nutrients at the Hubbard Brook Experimental Forest (HBEF) (1992–2023).

		Year		Year^2				
Species	n	estimate	p	estimate	p	Vertex	Δ_{vertex}	Δ_{total}
N (%)								
ACSA	112	**3.233 ± 1.172**	**0.01**	**−0.001 ± 0.0003**	**0.01**	2001	−0.40	−0.34
FAGR	107	**5.833 ± 1.094**	**<0.01**	**−0.002 ± 0.0003**	**<0.01**	2004	−0.55	−0.35
BEAL	112	**6.133 ± 1.408**	**<0.01**	**−0.002 ± 0.0004**	**<0.01**	2006	−0.45	−0.15
δ^{15}N (‰)								
ACSA	97	**−0.031 ± 0.007**	**<0.01**					−0.94
FAGR	96	−0.012 ± 0.007	0.08					
BEAL	100	−0.007 ± 0.007	0.30					
C (%)								
ACSA	112	**9.618 ± 4.108**	**0.02**	**−0.002 ± 0.001**	**0.02**	2003	−0.94	−0.63
FAGR	107	**−0.049 ± 0.012**	**<0.01**					−1.51
BEAL	112	**−0.046 ± 0.008**	**<0.01**					−1.42
C:N								
ACSA	112	**−45.207 ± 16.770**	**0.01**	**0.011 ± 0.004**	**0.01**	2000	5.81	5.02
FAGR	107	**−60.273 ± 16.770**	**<0.01**	**0.015 ± 0.003**	**<0.01**	2004	5.53	3.42
BEAL	112	**−50.746 ± 11.801**	**<0.01**	**0.013 ± 0.003**	**<0.01**	2007	3.39	0.69
P (ppm)								
ACSA	100	**2441.163 ± 980.419**	**0.01**	**−0.609 ± 0.244**	**0.01**	2005	−198.22	−96.05
FAGR	96	**−5.821 ± 2.389**	**0.02**					−181.07
BEAL	100	**5515.864 ± 1558.416**	**<0.01**	**−1.374 ± 0.388**	**<0.01**	2007	−338.72	−17.38
N:P								
ACSA	100	**−0.064 ± 0.021**	**<0.01**					−1.97
FAGR	95	**32.149 ± 14.425**	**0.03**	**−0.008 ± 0.004**	**0.03**	2007	−2.03	−0.22
BEAL	100	−0.029 ± 0.024	0.24					
δ^{13}C (‰)								
ACSA	96	−0.002 ± 0.009	0.84					
FAGR	91	**−12.738 ± 4.296**	**<0.01**	**0.003 ± 0.001**	**<0.01**	2013	0.38	−0.77
BEAL	96	**−9.070 ± 3.999**	**0.03**	**0.002 ± 0.001**	**0.03**	2013	0.21	−0.73
iWUE (μmol/mol)								
ACSA	96	**0.652 ± 0.093**	**<0.01**					19.55
FAGR	91	**−136.215 ± 47.128**	**<0.01**	**0.034 ± 0.012**	**<0.01**	2002	14.92	12.13
BEAL	96	**−98.687 ± 43.685**	**0.03**	**0.025 ± 0.011**	**0.03**	2000	13.55	12.49

Note: ACSA = sugar maple; FAGR = American beech; BEAL = yellow birch. Parameter estimates ± standard error and p values are shown for the best model. Parameters significant at $p < 0.05$ are in bold. n is the sample size. Vertex indicates the year the vertex occurred, if present. Δ_{vertex} and Δ_{total} indicate the change since the vertex and the total change over the record.

(Table 2; n = 22 years). Inclusion of the 3-year running average of N deposition or potential soil mineralization rates in July of the previous growing season as a predictor of mean annual foliar N was not supported for any species (Table 2).

Discussion

The foliar chemistry of the three co-dominant hardwood tree species at the HBEF responded to environmental changes in ways that largely support our hypotheses, with some important species-specific differences. For all three species, the declines in foliar N and C concentrations and increases in C:N ratios are consistent with expected long-term responses to both increasing CO_2 and decreasing N deposition in recent decades (e.g., Xu et al. 2020). Additionally, the declines in δ^{15}N and N:P ratio for sugar maple suggest a tightening of the N cycle and increasing N limitation over time. However, for American beech and yellow birch, foliar N:P ratios and δ^{15}N did not decrease significantly over the period of record. iWUE increased for all species, as expected from rising atmospheric CO_2, but increased the most for sugar maple.

Effects of declining atmospheric N deposition on foliar nutrients

Both N-addition experiments and measurements along gradients of N deposition show that foliar N is usually sensitive to increases in N inputs (Gundersen et al. 1998; Pardo et al. 2006; Crowley et al. 2012; Xu et al. 2020) but can lag changes in N inputs by several years (Gundersen et al. 1998). Foliar N measurements of canopy trees from Watershed 6 (adjacent to our study area) were conducted in 1965 and re-

Fig. 2. Trends in foliar C concentration (left) and C:N ratio (right) in co-dominant tree species at the Hubbard Brook Experimental Forest, 1992–2023. Solid lines indicate that coefficients were significant at $p < 0.05$. The line from the best fit model (linear vs. quadratic) is shown.

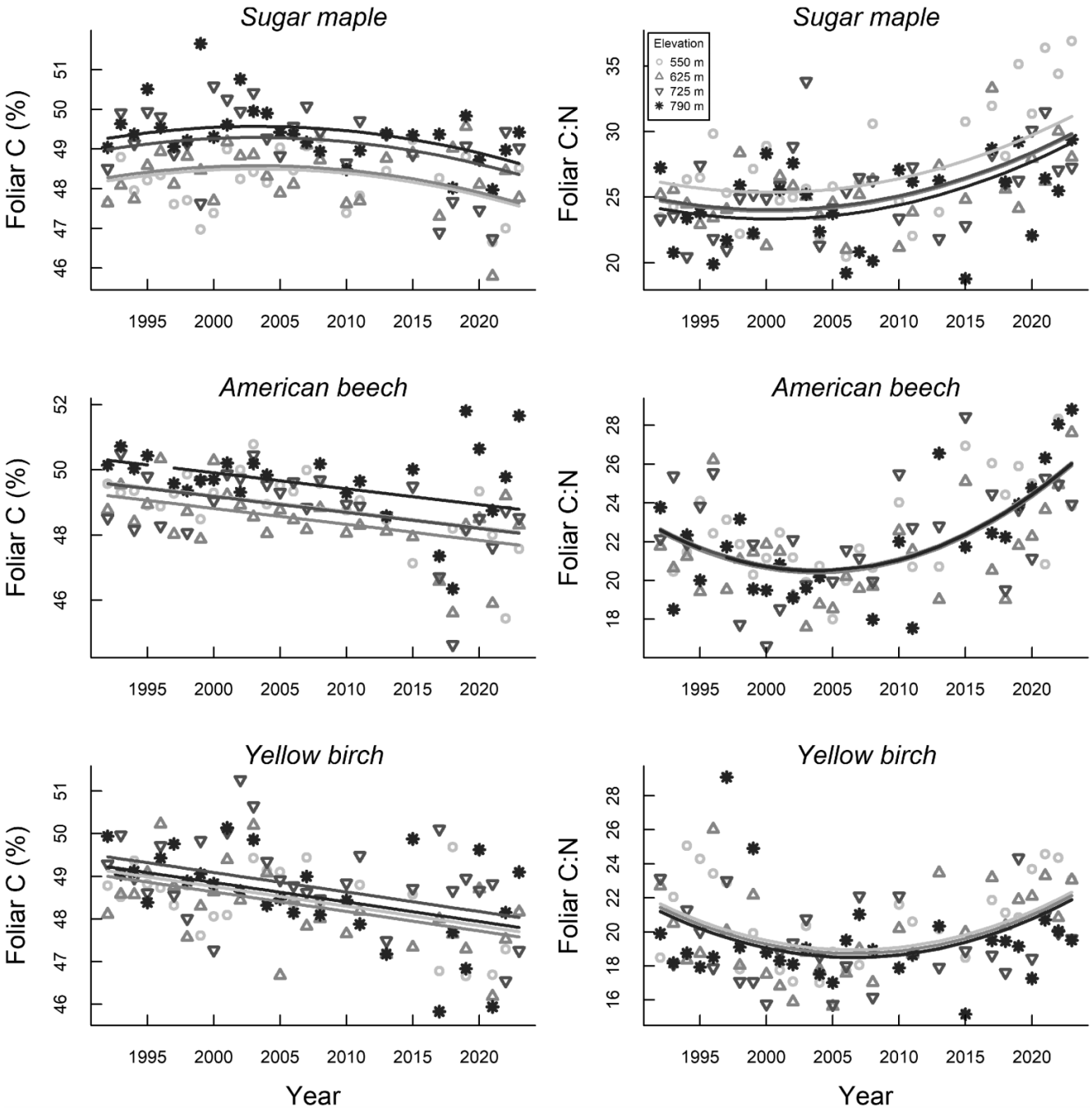

ported by Whittaker et al. (1979). Interestingly, pooled values from 1965 based on several representative trees from across the same elevation range as our study were similar to those we observed in 1992: sugar maple at 2.19%; American beech at 2.23%; yellow birch at 2.78% (Whittaker et al. 1979). In other studies, foliar N concentrations for the three focal tree species in this analysis increased significantly in response to both long-term (10 years), low-level (30 kg N ha^{-1} $year^{-1}$) experimental N additions at the HBEF and nearby forests (Zukswert et al. 2025), and along a N deposition gradient across the northeastern US (Pardo et al. 2006; Crowley et al. 2012). Changes in foliar N resulting from changes in N inputs are driven by changes in the amount of soil N available for plant uptake, along with possible additional direct uptake of N deposition through foliage (Guerrieri et al. 2011). Decreasing N inputs should have the opposite effect and lead to decreases in foliar N concentrations, again with some lag, as observed after cessation of experimental N additions (Högberg, et al. 2006; McNulty et al. 2017) and after experimental exclusion of high levels of N deposition in Europe (Gundersen et al. 1998). At the HBEF, bulk deposition of inorganic N was elevated throughout the late 20th cen-

Fig. 3. Trends in foliar P concentration (left) and N:P ratio (right) in co-dominant tree species at the Hubbard Brook Experimental Forest, 1992–2023. Solid lines indicate that coefficients were significant at $p < 0.05$. The line from the best fit model (linear vs. quadratic) is shown.

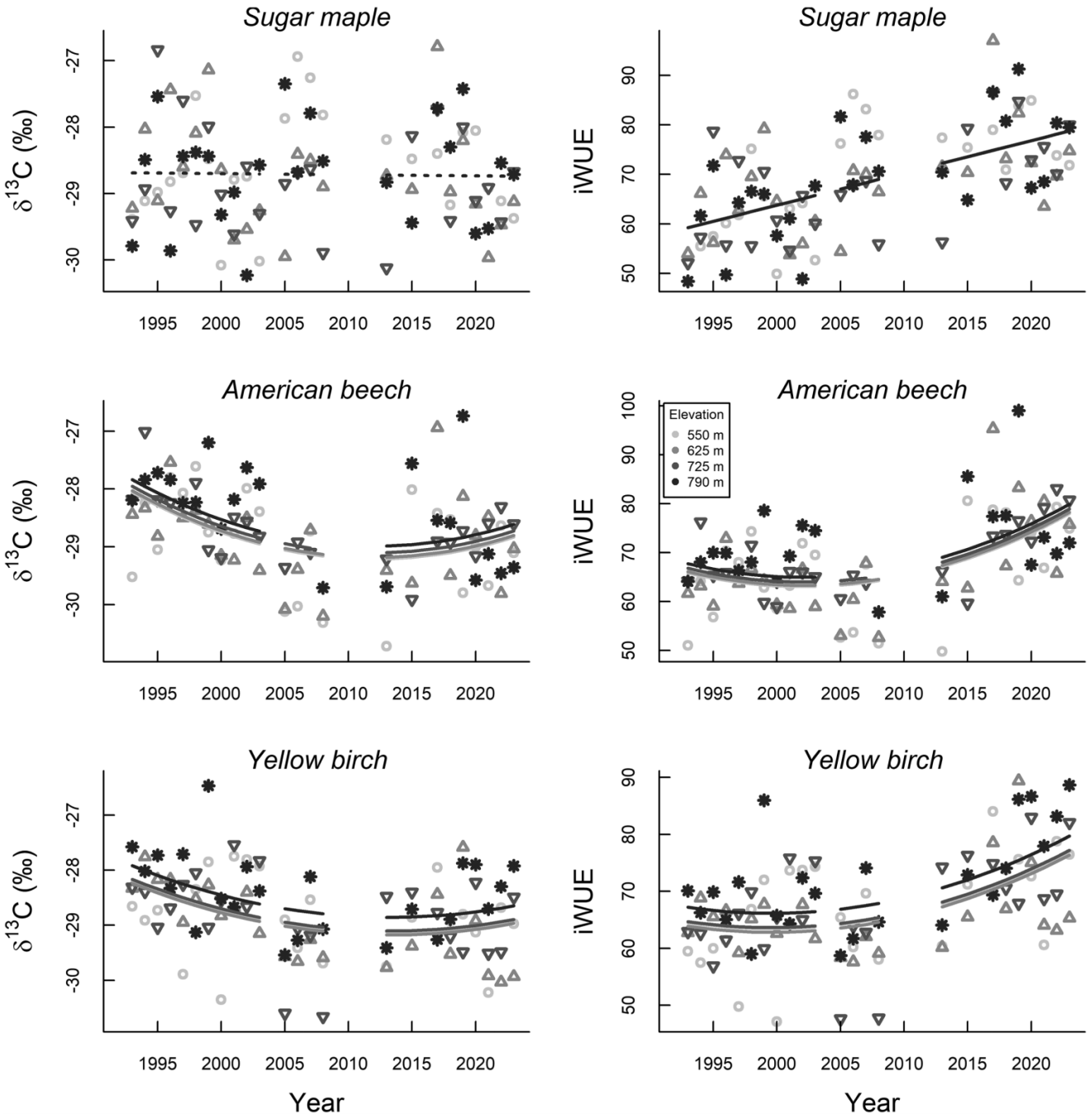

tury and then declined sharply over the first decade of the 21th century (Fig. S4), when foliar N started decreasing in all three species. The 3-year running average of N deposition was not directly related to foliar N in this study over the whole period of record, perhaps because the foliar N responses could lag deposition over periods longer than 3 years. This study's linear analyses of relationships between foliar N and its potential drivers would not fully capture hysteretic responses between ecosystem properties and N deposition as proposed by Gilliam et al. (2019), in which ecosystem lags could cause relationships between response variables and N deposition to differ between periods of increasing or chronically elevated N deposition and when deposition decreases.

Changes in N inputs can also alter foliar concentrations of other elements. Across the gradient of N deposition in the northeastern US, foliar P concentrations increased linearly with N deposition (e.g., Crowley et al. 2012), but experimental N and P additions at and near the HBEF showed that long-term N additions generally led to declines in foliar P (Zukswert et al. 2025). In this study, temporal declines in foliar P were modest, with no net shifts in N:P ratios over

Fig. 4. Trends in foliar $\delta^{13}C$ (left) and intrinsic water use efficiency (iWUE, right) in co-dominant tree species at the Hubbard Brook Experimental Forest, 1992–2023. Solid lines indicate that coefficients were significant at $p < 0.05$. The line from the best fit model (linear vs. quadratic) is shown.

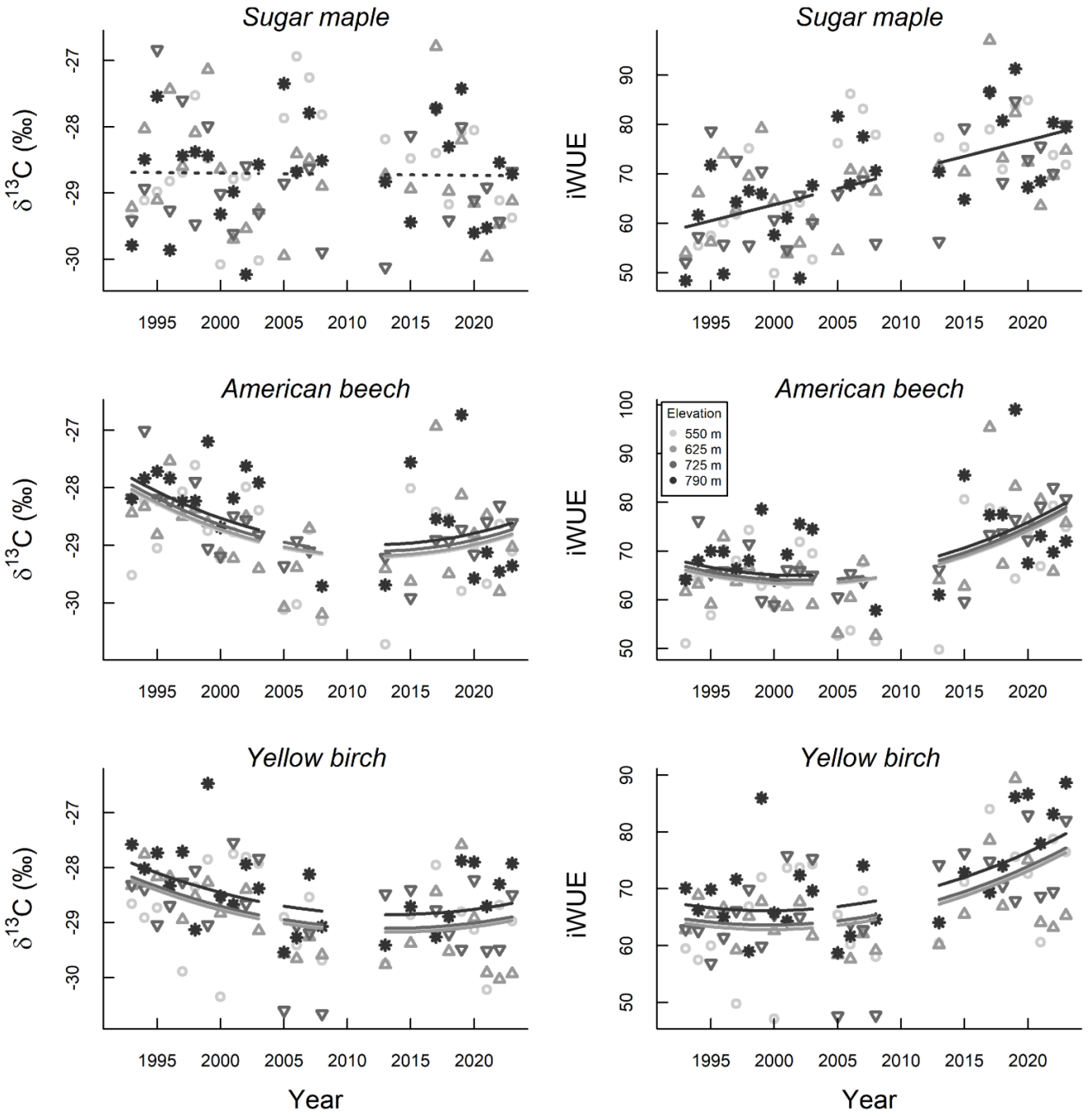

the study period for beech or yellow birch, and sugar maple N:P ratios decreased over time due to steeper declines in its N than P concentrations. Although it is possible to interpret this shift in N:P stoichiometry as a response to reduced N loading, elevated CO_2 also decreased plant N:P ratios in a global meta-analysis of global change experiments (Xu et al. 2020). In addition, this meta-analysis demonstrated that foliar C concentrations increase in response to N-addition experiments and tend to decrease in elevated CO_2 experiments (Xu et al. 2020), such that either rising CO_2 or falling N deposition could contribute to the decreasing foliar C concentrations observed in this study.

Effects of increasing atmospheric CO_2 concentration on foliar nutrients

Elevated CO_2 experiments regularly induce decreases in foliar concentrations of N and other nutrients (Cotrufo et al. 1998; Ainsworth and Long 2005; Xu et al. 2020). In trees across Europe, foliar N, P, and other nutrient concentrations decreased over the last three decades, correlating with increases

Table 2. Hypothesized correlates of average annual foliar nitrogen concentration (%).

Model	K	ACSA	FAGR	BEAL
Intercept only	2	6.55	4.45	**0.00**
CO_2 (ppm)	3	**0.00**	**0.00**	**0.20**
N deposition 3-year (kg N ha^{-1} $year^{-1}$)	3	6.16	2.28	2.95
Mineralization (mg N kg_{soil}^{-1} day^{-1})	3	7.59	3.22	6.14
Air temperature June–July (°C)	3	7.25	6.97	**1.72**
CO_2 estimate ± standard error		−0.006 ± 0.002	−0.006 ± 0.002	−0.003 ± 0.002
Air temperature estimate ± standard error				−0.034 ± 0.039

Note: Values are the difference in AIC corrected for sample size (ΔAICc) from the lowest AICc model. The lowest AICc model and all models within Δ2 AICc are in bold. For all models, n = 22 years. ACSA = sugar maple; FAGR = American beech; BEAL = yellow birch. K is the total number of model parameters.

in atmospheric CO_2 (Jonard et al. 2015; Penuelas et al. 2020). Several mechanisms have been proposed, including (1) dilution of foliar nutrients by increasing non-structural carbohydrates, (2) increased N use efficiency of photosynthesis, (3) downregulation of plant NO_3^- uptake in roots, (4) decreased nutrient transport to roots via mass flow, and (5) progressive N limitation at the ecosystem scale (Hilbert and Reynolds 1991; Luo et al. 2004; Taub and Wang 2008; Gojon et al. 2023; Perkowski et al. 2025). Below, we briefly discuss each of these hypothesized mechanisms, which are not mutually exclusive. The first four mechanisms could affect leaf N concentrations independent of soil N supply, as reported for both greenhouse experiments (Perkowski et al. 2025) and a large-scale set of field nutrient addition experiments (Cheaib et al. 2025). The fifth addresses the potential feedbacks to reducing foliar N through reduced soil N availability.

Increasing atmospheric CO_2 could dilute foliar N by increasing the sugar and starch concentration of plant tissues (Wolfe et al. 1998; Taub and Wang 2008). This CO_2-induced increase in non-structural carbohydrates is often accompanied by declines in structural C compounds, for an overall decrease in foliar C concentrations (Wolfe et al. 1998; Hobbie et al. 2002), as seen in this study (Table 1; Fig. 2). The second hypothesis maintains that plants downregulate investment in Rubisco as faster diffusion of CO_2 into leaves and suppressed photorespiration from elevated CO_2 allow for increased efficiency in using these N-rich enzymes (Smith and Keenan 2020; Smith et al. 2024; Perkowski et al. 2025). The third hypothesis, still not fully understood, is that elevated CO_2 can cause downregulation of the activity of membrane transporters involved in root NO_3^- uptake (Taub and Wang 2008; Gojon et al. 2023) and can impede NO_3^- reduction and assimilation into organic N within the plant (Bloom et al. 2012; Feng et al. 2015). These mechanisms are difficult to assess in this study, however, as the form and rate of root N uptake are not regularly measured at the HBEF.

The fourth hypothesis proposes that CO_2-driven decreases in stomatal conductance and transpiration could reduce the mass flow of nutrients to the roots and through stems, a process that should be especially important for macronutrients supplied primarily by mass flow such as Ca, Mg, and sometimes NO_3^- (Taub and Wang 2008), but less important for nutrients supplied by diffusion or mycorrhizal fungi such as P and NH_4^+. At the HBEF, foliar $\delta^{13}C$ measurements do indicate that iWUE has increased (Fig. 4), which could be driven by an increase in photosynthesis or a decrease in stomatal conductance. However, a CO_2-driven decrease in nutrient flow via transpiration cannot explain the foliar N declines in this study, because measurements of catchment water budgets at the HBEF show that rather than decreasing over time along with rising atmospheric CO_2, evapotranspiration remained relatively steady over decades until abruptly increasing by ~30% for 2010–2019 (Green et al. 2021).

At the ecosystem scale, elevated CO_2 is expected to reduce soil nutrient availability and cause progressive N limitation because of both nutrient accumulation in stimulated production of plant biomass and increased nutrient immobilization in soils as plants produce litter with higher C:N ratios (Luo et al. 2004). At the HBEF, since the early 1980s, the nutrient stock in above-ground plant biomass has been roughly constant rather than accumulating (van Doorn et al. 2011; Battles et al. 2014), and thus is unlikely to drive progressive N limitation or explain declines in foliar N. However, foliar C:N ratio increased in all three dominant tree species (Fig. 2). If leaf litterfall C:N increased as well, this material should immobilize markedly more N in decomposing litter and delay the release of N and other nutrients via mineralization, which could reduce plant N uptake and further reduce foliar N concentrations, and soil net N mineralization rates at the HBEF have declined over the last several decades (Durán et al. 2016; Wilson et al. 2025).

Multiple drivers of foliar N trends

Overall, both decreasing N deposition and rising atmospheric CO_2 are expected to reduce foliar nutrient concentrations in the ways we observed at the HBEF, but because these hypothesized drivers are highly correlated over time, they cannot be disentangled in this study. Factors such as stand age and canopy decline also changed over time and could contribute to the observed patterns in foliar N. The sample trees in our study increased in age from roughly 80 years at the beginning to 110 years, and canopy decline and dieback have occurred in the study area for both sugar maple (Juice et al. 2006) and American beech, the latter owing to progression of beech bark disease (Cleavitt et al. 2022). Yet, several studies report no changes in foliar N with stand age across a wide chronosequence of stand ages (Binkley et al. 1995; Clinton et al. 2002; Liang et al. 2018), or between mid-successional and

mature trees of our three focal species (Zukswert et al. 2025). Along a gradient of beech bark disease damage in the Catskill Mountains, New York, foliar N concentrations increased for sugar maple but did not change for beech (Lovett et al. 2010), and so beech bark disease appears unlikely explain the declines in foliar N observed in three species in this study. However, foliar N of declining sugar maple has been shown to be lower than for healthy trees (Mader and Thompson 1969).

Effects of air temperature and soil N availability on foliar N and δ^{15}N patterns along the elevation gradient

Along the 240 m elevation gradient in this study, foliar N concentrations increased a small amount for sugar maple and yellow birch, while beech foliar N did not vary with elevation. This is mostly consistent with a study of sugar maple and American beech along a larger (390 m) elevation gradient elsewhere at the HBEF, which found that foliar N concentrations increased for sugar maple but were mixed for American beech along the gradient (Fahey et al. 2025*a*). In this study, foliar δ^{15}N showed large (1.2–1.5 ‰) and consistent increases with elevation for all three species. Potential factors that might drive these foliar responses that also varied with elevation along this gradient include a decrease in annual mean temperature by 1.5 °C, an increase in mean annual precipitation of 77 mm along with associated N deposition, and an increase in potential soil N mineralization rates (Bohlen et al. 2001; Durán et al. 2016).

Globally, foliar N concentrations generally increase with increasing latitude and elevation, allowing plants to compensate for reduced rates of biochemical processes at cooler temperatures (Reich and Oleksyn 2004). Conversely, plants can acclimate to warming temperatures with decreased foliar N concentrations (Haxeltine and Prentice 1996). The small increases in foliar N with elevation in this study are consistent with these global responses to spatial variations in air temperature, but other factors could also contribute. Unlike for foliar N, the patterns of increasing foliar δ^{15}N with elevation in this study were the opposite direction of responses with temperature reported for both global temperature gradients (Amundson et al. 2003) and in a warming study at the HBEF (Harrison et al. 2020), where foliar δ^{15}N increased with warmer rather than cooler temperatures. Notably, foliar δ^{15}N did not increase with temperature at 51 sites across northeastern North America (Pardo et al. 2006), indicating that regional patterns can deviate from global observations. The increase in precipitation with elevation is unlikely to have greatly affected foliar N and δ^{15}N. The precipitation increase was small (5%), and a corresponding 5% increase in N deposition (less than 0.3 kg N ha^{-1} year^{-1}) should have had negligible effects on foliar N and δ^{15}N.

Elevational patterns of both foliar N and δ^{15}N were consistent with variations in soil N cycling across the elevation gradient in this study. At the HBEF, the bedrock-dominated upper portions of the catchment are hotspots for nitrate production and denitrification, and soils have higher δ^{15}N values than the lower portions (Roco et al. 2019; Pardo et al. 2022). Thus, the elevational patterns in foliar N and δ^{15}N at the HBEF may reflect the patterns in soil type and increasing potential mineralization and nitrification along the elevation gradient (Bohlen et al. 2001), which lead to denitrification, and nitrate export and soils that are enriched in δ^{15}N. The directionally consistent responses of both foliar N and δ^{15}N with soil N cycling along the elevation gradient in this study may reflect a stronger role for soil N than air temperature as a driver of these foliar patterns.

Foliar δ^{15}N temporal trends and species differences

Plant δ^{15}N is often expected to decrease in response to increasing soil N limitation, and with increasing plant reliance on mycorrhizal-mediated N uptake. That is, nitrification and denitrification preferentially consume ^{14}N over ^{15}N, so δ^{15}N accumulates within the ecosystem, and can be reflected in increasing plant δ^{15}N as these loss processes increase with increasing soil N availability (e.g., Högberg 1998; Pardo et al. 2006; Sabo et al. 2020). In addition, mycorrhizal-mediated N uptake often fractionates against ^{15}N, and plants should increasingly rely on mycorrhizal uptake as soil N becomes more limiting. Plants with ectomycorrhizal associations should fractionate more against ^{15}N than plants with arbuscular mycorrhizal associations (Hobbie and Ouimette 2009), and ectomycorrhizal species should experience larger increases in fractionation as soil N availability decreases (e.g., Hobbie et al. 2005).

N mineralization rates have decreased over the study period at the HBEF (Wilson et al. 2025), which might be expected to drive declines in foliar δ^{15}N in all three species, especially the two ectomycorrhizal species, beech and yellow birch. However, foliar δ^{15}N declined over time only for sugar maple, a species that forms arbuscular mycorrhizal associations, and not for beech or yellow birch (Fig. 1), responses that contradicted expectations based on mycorrhizal differences. However, they were consistent with the responses of these same three species over the gradient of N deposition across the northeastern US, where foliar δ^{15}N for sugar maple increased significantly with N deposition, as well as for the ectomycorrhizal species red oak (*Quercus rubra* L.), red spruce, eastern hemlock (*Tsuga canadensis* (L.) Carriére), and balsam fir, but not for beech and yellow birch (Pardo et al. 2006). The reasons for the lack of foliar δ^{15}N response to N availability by beech and yellow birch are not readily apparent.

The dominant form of N uptake may differ among the three focal species in this study, with possible consequences for foliar δ^{15}N trends. As a species with arbuscular mycorrhizal associations, sugar maple should rely more on inorganic N than beech or yellow birch, which are ectomycorrhizal and should rely more on N from soil organic matter (Phillips et al. 2013). Consequently, sugar maple should be more sensitive to changes in inorganic N availability and could be particularly sensitive to change in NO_3^-. Although all three tree species generally prefer NH_4^+ over NO_3^- (Templer and Dawson 2004), soils under sugar maple often promote high rates of nitrification and have higher soil NO_3^- concentrations (Lovett et al. 2004), and so sugar maple should regularly encounter more soil NO_3^- than do beech or yellow birch. Nitrification can be

highly fractionating, producing ^{15}N-depleted NO_3^- and enriching the residual NH_4^+ source pool (e.g., Högberg 1998). Greater reliance on NO_3^-, combined with large declines in soil NO_3^- production and export in recent decades (Wilson et al. 2025), might contribute to the downward trend in sugar maple foliar $\delta^{15}N$, but not in beech and yellow birch if they rely more on organic N sources.

Foliar $\delta^{15}N$ could also partly reflect the isotopic composition of its N sources. Nitrate made up almost two-thirds of total bulk deposition at the HBEF averaged over the study period and was responsible for much of the decline in N deposition. Its $\delta^{15}N$ composition was not measured routinely, but it averaged -2.5 ± 2.0‰ across several studies at the HBEF (Pardo et al. 2004; Wexler et al. 2014; Sebestyen et al. 2019). Ammonium made up the rest of the bulk N deposition, but its $\delta^{15}N$ has not been measured at Hubbard Brook. In central Maine, mean annual $\delta^{15}N$–NH_4^+ in precipitation averaged -1.2 ± 1.0‰ (Downs et al. 1999). However, accumulation of either form of N from deposition probably did not contribute to the decline in foliar $\delta^{15}N$ in sugar maple, which became isotopically lighter than both of these N sources over the study period.

Intrinsic water use efficiency

The declines in $\delta^{13}C$ observed for American beech and yellow birch, but not sugar maple, translated to greater increases in iWUE over time for sugar maple than the other two canopy species. One possible reason for these species' differences could be whether stomatal conductance decreased for sugar maple but not American beech or yellow birch. However, elevated CO_2 did not affect stomatal conductance for sugar maple in elevated CO_2 experiments (Roth et al. 1997; St.Clair et al. 2008). Another possibility is that carbon assimilation increased over time more for sugar maple than the other tree species. Photosynthesis has not been directly measured over time at Hubbard Brook, but a greater increase in carbon assimilation for sugar maple than American beech or yellow birch is unlikely given the observed depressed growth of sugar maple in the Hubbard Brook forest in recent decades (Battles et al. 2014); moreover, sugar maple basal area in the study area has declined since 1997, while total forest basal area has been stable or slightly increasing (Cleavitt et al. 2021). Nutrient availability can also affect foliar $\delta^{13}C$, but decreasing N availability seems unlikely to explain species' temporal trends in foliar $\delta^{13}C$ or iWUE (Fig. 4). In a long-term N fertilization experiment at Hubbard Brook and nearby forests, foliar $\delta^{13}C$ increased for sugar maple, but not for beech or yellow birch (Zukswert et al. 2024). Thus, we expected increased N limitation over time in our study to be accompanied by decreased foliar $\delta^{13}C$ in sugar maple but not the other two species, which is the opposite species pattern from what we observed, indicating that other controls on foliar $\delta^{13}C$ must be more important than effects of N.

The increase in iWUE, especially after approximately 2010, combined with the abrupt increase in ET at the HBEF starting in 2010 (Green et al. 2021), suggests an increase in carbon assimilation and gross primary production that is not reflected in aboveground biomass, which has remained nearly constant (van Doorn et al. 2011; Battles et al. 2014; Cleavitt et al. 2021). However, an abrupt increase in soil respiration has been observed in the past decade at the HBEF and nearby forests (Mann et al. 2024; Possinger et al. 2025), and both low soil N availability (Bae et al. 2015) and enhanced demand for nutrients with increased photosynthesis due to elevated CO_2 (Hilbert and Reynolds 1991; Franklin 2007) can increase belowground carbon allocation. It will be important for future studies to quantify ecosystem-scale changes in the water cycle, biomass accumulation, and soil respiration due to increasing CO_2, possibly coupled with progressive nitrogen limitation, to better understand how forests respond to these environmental changes. Future studies could collect data on $\delta^{18}O$ to disentangle contributions to changes in iWUE from transpiration, as ^{18}O enrichment indicates changes in transpiration and water use independent of photosynthesis (Guerrieri et al. 2011, 2019).

Implications for ecosystem processes

Ecosystem-scale responses to both changing N deposition and rising CO_2 may occur over time through plant–soil feedbacks (Groffman et al. 2018; Mason et al. 2022) and affect higher trophic levels as well. The progressive N limitation hypothesis holds that N availability in the soil should decrease over time as elevated CO_2 stimulates plant growth and increases the amount of N accumulated in plant biomass and soil organic matter pools, while increased C:N of foliage and litter increases microbial N immobilization, which further reduces soil N availability to plants (Luo et al. 2004). Reductions in N deposition and increasing N demands over a longer growing season could further exacerbate this N limitation (Rastetter et al. 1997; Reich et al. 2006; Norby et al. 2009; Coskun et al. 2016; Groffman et al. 2018), and long-term measurements show reductions in soil N availability at the HBEF (Durán et al. 2016; Wilson et al. 2025). This study provides evidence of declines in foliar N concentrations (Fig. 1) and increases in foliar C:N ratios (Fig. 2) for all three dominant tree species, trends that are likely responding to and amplifying declines in soil N availability through increased N immobilization and delayed N mineralization. Foliar N content is an important indicator of food nutritional quality for herbivores (Mattson 1980), and these declines in foliar N and changing nutrient ratios may have further cascading effects on the distribution of biomass among producers and consumers (i.e., trophic structure) in forest ecosystems (Cebrian et al. 2009).

Acknowledgements

We would like to thank Ian Halm for years of tree climbing, Cindy Wood and Suzanne Wapner for coordinating collections 1992–2013, Jane Hislop and Jeff Merriam for USFS lab coordination 2013–2023, Paul Brooks and Stefania Mambelli for Berkeley lab coordination, and Geoff Wilson, Amey Bailey, Adam Wild, Anthony Stewart, and many others for foliage collection. The Hubbard Brook Experimental Forest is maintained and operated by Northern Research Station, United States Department of Agriculture Forest Service, Madison, Wisconsin, United States.

Article information

History dates

Received: 4 April 2025
Accepted: 23 December 2025
Accepted manuscript online: 14 January 2026
Version of record online: 23 February 2026

Notes

This paper is part of a collection celebrating Tim Fahey's career and contributions to forest ecology.

Data availability

Atmospheric CO_2 and atmospheric $\delta^{13}C$ (Keeling et al. 2005) were downloaded from https://scrippsco2.ucsd.edu/data/atmospheric_co2/mlo.html. All other data analyzed in this study are available in the Environmental Data Initiative data repository. Datasets are cited within the text, and additionally are cited here:

Fahey, T.J., Pardo, L.H., Goodale, C.L., Lany, N.K., Cleavitt, N., 2025. Hubbard Brook Experimental Forest: Watershed 6 Temporal Canopy Leaf Chemistry, 1992—ongoing ver 7. Environmental Data Initiative. https://doi.org/10.6073/pasta/2d9681b7c31dd92c90b67934bd105e5a.

USDA Forest Service, Northern Research Station 2025. Hubbard Brook Experimental Forest: Daily Temperature Record, 1955—present ver 15. Environmental Data Initiative. https://doi.org/10.6073/pasta/e698e823085c4edcb7d59b4b7d945b49.

USDA Forest Service, Northern Research Station 2024. Hubbard Brook Experimental Forest: Daily Precipitation Rain Gage Measurements, 1956—present ver 22. Environmental Data Initiative. https://doi.org/10.6073/pasta/e55baf46bd1c49b38a5806f15fa54801.

Groffman, P.M., Martel, L.D., 2025. Long-term measurements of microbial biomass and activity at the Hubbard Brook Experimental Forest 1994—ongoing ver 25. Environmental Data Initative. https://doi.org/10.6073/pasta/aff4a2074fd56102f62f13a19ce46f2d.

Hubbard Brook Watershed Ecosystem Record (HBWatER), 2024. Hubbard Brook Experimental Forest: Chemistry of Precipitation—Monthly Fluxes, Watershed 6, 1964—ongoing ver 12. Environmental Data Initiative. https://doi.org/10.6073/pasta/daf8b920308b18f595a1aaa014b37021.

Keeling, C.D., Piper, S.C., Bacastow, R.B., Wahlen, M., Whorf, T.P., Heimann, M., Meijer, H.A., 2005. Atmospheric CO_2 and $^{13}CO_2$ Exchange with the Terrestrial Biosphere and Oceans from 1978 to 2000: Observations and Carbon Cycle Implications, in: Baldwin, I.T., Caldwell, M.M., Heldmaier, G., Jackson, R.B., Lange, O.L., Mooney, H.A., Schulze, E.-D., Sommer, U., Ehleringer, J.R., Denise Dearing, M., Cerling, T.E. (Eds.), A History of Atmospheric CO_2 and Its Effects on Plants, Animals, and Ecosystems. Springer New York, New York, NY, pp. 83–113. https://doi.org/10.1007/0-387-27048-5_5.

Author information

Author ORCIDs

Nina K. Lany https://orcid.org/0000-0003-0868-266X
Natalie L. Cleavitt https://orcid.org/0000-0003-0425-2486
Christine L. Goodale shttps://orcid.org/0000-0003-4317-3983

Author notes

Natalie L. Cleavitt served as Guest Editor of the "Celebration of Tim Fahey's career and contributions to Forest Ecology" collection at the time of manuscript review and acceptance; peer review and editorial decisions regarding this manuscript were handled by another editorial board member.

Author contributions

Conceptualization: NKL, LHP, TJF, CLG
Data curation: NKL, LHP, TJF, CLG
Formal analysis: NKL
Methodology: NKL, LHP, NLC, TJF, CLG
Writing – original draft: NKL, LHP, CLG
Writing – review & editing: NKL, LHP, NLC, TJF, CLG

Competing interests

The authors declare there are no competing interests.

Funding information

Funding for this study was provided by the Northern Research Station, United States Department of Agriculture Forest Service and the National Science Foundation through the Directorate for Biological Sciences, Long-Term Ecological Research (LTER) Program, grant/award numbers: 9211768, 9810221, 0423259, 1114804, 1637685, 2224545.

Supplementary material

Supplementary data are available with the article at https://doi.org/10.1139/cjfr-2025-0105.

References

Aerts, R. 1996. Nutrient resorption from senescing leaves of perennials: are there general patterns? J. Ecol. **84**: 597–608. doi:10.2307/2261481.

Ainsworth, E.A., and Long, S.P. 2005. What have we learned from 15 years of free-air CO_2 enrichment (FACE)? A meta-analytic review of the responses of photosynthesis, canopy properties and plant production to rising CO_2. New Phytol. **165**: 351–372. doi:10.1111/j.1469-8137.2004.01224.x.

Amundson, R., Austin, A.T., Schuur, E.A.G., Yoo, K., Matzek, V., Kendall, C., et al. 2003. Global patterns of the isotopic composition of soil and plant nitrogen. Glob. Biogeochem. Cycles, **17**. doi:10.1029/2002GB001903.

Bae, K., Fahey, T.J., Yanai, R.D., and Fisk, M. 2015. Soil nitrogen availability affects belowground carbon allocation and soil respiration in Northern Hardwood Forests of New Hampshire. Ecosystems, **18**: 1179–1191. doi:10.1007/s10021-015-9892-7.

Bailey, S.W., McGuire, K.J., Ross, D.S., Green, M.B., and Fraser, O.L. 2019. Mineral weathering and podzolization control acid neutralization and streamwater chemistry gradients in upland glaciated catchments, Northeastern United States. Front. Earth Sci. **7**. doi:10.3389/feart.2019.00063.

Battles, J.J., Fahey, T.J., Driscoll, C.T.J. r., Blum, J.D., and Johnson, C.E. 2014. Restoring soil calcium reverses forest decline. Environ. Sci. Technol. Lett. **1**: 15–19. doi:10.1021/ez400033d.

Binkley, D., Smith, F.W., and Son, Y. 1995. Nutrient supply and declines in leaf area and production in lodgepole pine. Can. J. For. Res. **25**: 621–628. doi:10.1139/x95-069.

Bloom, A.J., Asensio, J.S.R., Randall, L., Rachmilevitch, S., Cousins, A.B., and Carlisle, E.A. 2012. CO_2 enrichment inhibits shoot nitrate assimilation in C_3 but not C_4 plants and slows growth under nitrate in C_3 plants. Ecology, **93**: 355–367. doi:10.1890/11-0485.1.

Bohlen, P.J., Groffman, P.M., Driscoll, C.T., Fahey, T.J., and Siccama, T.G. 2001. Plant–soil–microbial interactions in a northern hardwood forest. Ecology, **82**: 965–978. doi:10.1890/0012-9658(2001)082[0965:PSMIIA]2.0.CO;2.

Burnham, K.P., and Anderson, D.R. 2004. Multimodel inference: understanding AIC and BIC in model selection. Sociol. Methods Res. **33**: 261–304. doi:10.1177/0049124104268644.

Buso, D.C., Likens, G.E., and Eaton, J.S. 2000. Chemistry of precipitation, streamwater, and lakewater from the Hubbard Brook Ecosystem Study: a record of sampling protocols and analytical procedures. U.S. Department of Agriculture, Forest Service, Northeastern Research Station. doi:10.2737/ne-gtr-275.

Cebrian, J., Shurin, J.B., Borer, E.T., Cardinale, B.J., Ngai, J.T., Smith, M.D., and Fagan, W.F. 2009. Producer nutritional quality controls ecosystem trophic structure. PLoS One, **4**: e4929. doi:10.1371/journal.pone.0004929.

Cheaib, A., Waring, E.F., McNellis, R., Perkowski, E.A., Martina, J.P., Seabloom, E.W., et al. 2025. Soil nitrogen supply exerts largest influence on leaf nitrogen in environments with the greatest leaf nitrogen demand. Ecol. Lett. **28**: e70015. doi:10.1111/ele.70015.

Cleavitt, N.L., Battles, J.J., Fahey, T.J., and van Doorn, N.S. 2021. Disruption of the competitive balance between foundational tree species by interacting stressors in a temperate deciduous forest. J. Ecol. **109**: 2754–2768. doi:10.1111/1365-2745.13687.

Cleavitt, N.L., Montague, M.S., Battles, J.J., Box, O.F., Matthes, J.H., and Fahey, T.J. 2022. Enemy release from beech bark disease coincides with upslope shift of American beech. Can. J. For. Res. **52**: 1224–1233. doi:10.1139/cjfr-2022-0107.

Clinton, P.W., Allen, R.B., and Davis, M.R. 2002. Nitrogen storage and availability during stand development in a New Zealand Nothofagus forest. Can. J. For. Res. **32**: 344–352. doi:10.1139/x01-188.

Coskun, D., Britto, D.T., and Kronzucker, H.J. 2016. Nutrient constraints on terrestrial carbon fixation: the role of nitrogen. J. Plant Physiol. **203**: 95–109. doi:10.1016/j.jplph.2016.05.016.

Cotrufo, M.F., Ineson, P., and Scott, Y. 1998. Elevated CO_2 reduces the nitrogen concentration of plant tissues. Glob. Change Biol. **4**: 43–54. doi:10.1046/j.1365-2486.1998.00101.x.

Crowley, K.F., McNeil, B.E., Lovett, G.M., Canham, C.D., Driscoll, C.T., Rustad, L.E., et al. 2012. Do nutrient limitation patterns shift from nitrogen toward phosphorus with increasing nitrogen deposition across the Northeastern United States? Ecosystems, **15**: 940–957. doi:10.1007/s10021-012-9550-2.

Downs, M., Michener, R., Fry, B., and Nadelhoffer, K. 1999. Routine measurement of dissolved inorganic ^{15}N in precipitation and streamwater. Environ. Monit. Assess. **55**: 211–220. doi:10.1023/A:1006194307747.

Driscoll, C., Milford, J.B., Henze, D.K., and Bell, M.D. 2024. Atmospheric reduced nitrogen: sources, transformations, effects, and management. J. Air Waste Manage. Assoc. **74**: 362–415. doi:10.1080/10962247.2024.2342765.

Durán, J., Morse, J.L., Groffman, P.M., Campbell, J.L., Christenson, L.M., Driscoll, C.T., et al. 2016. Climate change decreases nitrogen pools and mineralization rates in northern hardwood forests. Ecosphere, **7**: e01251. doi:10.1002/ecs2.1251.

Fahey, T.J., Cleavitt, N.L., and Battles, J.J. 2022. Long term variation of leaf abundance in a northern hardwood forest. Ecol. Indic. **137**: 108746. doi:10.1016/j.ecolind.2022.108746.

Fahey, T.J., Cleavitt, N.L., Templer, P.H., Groffman, P.M., Bailey, A.S., Caron, S.B., and Wilson, G. 2025a. Foliar resorption of beech and maple along an elevation gradient in a northern hardwood forest. For. Ecosyst. **13**: 100304. doi:10.1016/j.fecs.2025.100304.

Fahey, T.J., Pardo, L.H., Goodale, C.L., Lany, N.K., and Cleavitt, N., 2025b. Hubbard Brook Experimental Forest: Watershed 6 Temporal Canopy Leaf Chemistry, 1992—ongoing ver 7. Environmental Data Initiative. doi:10.6073/pasta/2d9681b7c31dd92c90b67934bd105e5a.

Farquhar, G.D., O'Leary, M.H., and Berry, J.A. 1982. On the relationship between carbon isotope discrimination and the intercellular carbon dioxide concentration in leaves. Funct. Plant Biol. **9**: 121–137.

Farquhar, G.D., Ehleringer, J.R., and Hubick, K.T. 1989. Carbon isotope discrimination and photosynthesis. Annu. Rev. Plant Biol. **40**: 503–537. doi:10.1146/annurev.pp.40.060189.002443.

Feng, Z., Rütting, T., Pleijel, H., Wallin, G., Reich, P.B., Kammann, C.I., et al. 2015. Constraints to nitrogen acquisition of terrestrial plants under elevated CO_2. Global Change Biol. **21**: 3152–3168. doi:10.1111/gcb.12938.

Franklin, O. 2007. Optimal nitrogen allocation controls tree responses to elevated CO_2. New Phytol. **174**: 811–822. doi:10.1111/j.1469-8137.2007.02063.x.

Gilliam, F.S., Burns, D.A., Driscoll, C.T., Frey, S.D., Lovett, G.M., and Watmough, S.A. 2019. Decreased atmospheric nitrogen deposition in eastern North America: predicted responses of forest ecosystems. Environ. Pollut. **244**: 560–574. doi:10.1016/j.envpol.2018.09.135.

Gojon, A., Cassan, O., Bach, L., Lejay, L., and Martin, A. 2023. The decline of plant mineral nutrition under rising CO_2: physiological and molecular aspects of a bad deal. Trends Plant Sci. **28**: 185–198. doi:10.1016/j.tplants.2022.09.002.

Green, M.B., Bailey, S.W., Campbell, J.L., McGuire, K.J., Bailey, A.S., Fahey, T.J., et al. 2021. A catchment water balance assessment of an abrupt shift in evapotranspiration at the Hubbard Brook Experimental Forest, New Hampshire, USA. Hydrol. Process. **35**: e14300. doi:10.1002/hyp.14300.

Groffman, P.M., and Martel, L.D. 2025. Long-term measurements of microbial biomass and activity at the Hubbard Brook Experimental Forest 1994—ongoing ver 25. Environmental Data Initative. doi:10.6073/pasta/aff4a2074fd56102f62f13a19ce46f2d.

Groffman, P.M., Driscoll, C.T., Durán, J., Campbell, J.L., Christenson, L.M., Fahey, T.J., et al. 2018. Nitrogen oligotrophication in northern hardwood forests. Biogeochemistry, **141**: 523–539. doi:10.1007/s10533-018-0445-y.

Guerrieri, R., Menuccini, M., Sheppard, L.J., Saurer, M., Perks, M.P., Levy, P., et al. 2011. The legacy of enhanced N and S deposition as revealed by the combined analysis of $\delta^{13}C$, $\delta^{18}O$ and $\delta^{15}N$ in tree rings. Global Change Biol. **17**: 1946–1962. doi:10.1111/j.1365-2486.2010.02362.x.

Guerrieri, R., Lepine, L., Asbjornsen, H., Xiao, J., and Ollinger, S.V. 2016. Evapotranspiration and water use efficiency in relation to climate and canopy nitrogen in U.S. forests. J. Geophys. Res. Biogeosci. **121**: 2610–2629. doi:10.1002/2016JG003415.

Guerrieri, R., Belmecheri, S., Ollinger, S.V., Asbjornsen, H., Jennings, K., Xiao, J., et al. 2019. Disentangling the role of photosynthesis and stomatal conductance on rising forest water-use efficiency. Proc. Natl. Acad. Sci. **116**: 16909–16914. doi:10.1073/pnas.1905912116.

Gundersen, P., Emmett, B.A., Kjønaas, O.J., Koopmans, C.J., and Tietema, A. 1998. Impact of nitrogen deposition on nitrogen cycling in forests: a synthesis of NITREX data. For. Ecol. Manage. **101**: 37–55. doi:10.1016/S0378-1127(97)00124-2.

Harrison, J.L., Schultz, K., Blagden, M., Sanders-DeMott, R., and Templer, P.H. 2020. Growing season soil warming may counteract trend of nitrogen oligotrophication in a northern hardwood forest. Biogeochemistry, **151**: 139–152. doi:10.1007/s10533-020-00717-z.

Haxeltine, A., and Prentice, I.C. 1996. A general model for the light-use efficiency of primary production. Funct. Ecol. **10**: 551–561. doi:10.2307/2390165.

Hilbert, D., and Reynolds, J.F. 1991. A model allocating growth among leaf proteins, shoot structure, and root biomass to produce balanced activity. Ann. Bot. **68**: 417–425. doi:10.1093/oxfordjournals.aob.a088273.

Hobbie, E.A., and Ouimette, A.P. 2009. Controls of nitrogen isotope patterns in soil profiles. Biogeochemistry, **95**: 355–371. doi:10.1007/s10533-009-9328-6.

Hobbie, E.A., Gregg, J., Olszyk, D.M., Rygiewicz, P.T., and Tingey, D.T. 2002. Effects of climate change on labile and structural carbon in Douglas-fir needles as estimated by $\delta^{13}C$ and C_{area} measurements. Global Change Biol. **8**: 1072–1084. doi:10.1046/j.1365-2486.2002.00541.x.

Hobbie, E.A., Jumpponen, A., and Trappe, J. 2005. Foliar and fungal ^{15}N:^{14}N ratios reflect development of mycorrhizae and nitrogen sup-

ply during primary succession: testing analytical models. Oecologia, **146**: 258–268. doi:10.1007/s00442-005-0208-z.

Högberg, P. 1998. Tansley Review No. 95: ^{15}N natural abundance in soil–plant systems. New Phytol. **139**: 595–595. doi:10.1046/j.1469-8137.1998.00239.x.

Högberg, P., Fan, H., Quist, M., Binkley, D., and Tamm, C.O. 2006. Tree growth and soil acidification in response to 30 years of experimental nitrogen loading on boreal forest. Global Change Biol. **12**: 489–499. doi:10.1111/j.1365-2486.2006.01102.x.

Hubbard Brook Watershed Ecosystem Record (HBWatER). 2024. Hubbard Brook Experimental Forest: Chemistry of Precipitation—Monthly Fluxes, Watershed 6, 1964—ongoing ver 12. Environmental Data Initiative. doi:10.6073/pasta/daf8b920308b18f595a1aaa014b37021.

Johnson, C.E., Driscoll, C.T., Siccama, T.G., and Likens, G.E. 2000. Element fluxes and landscape position in a northern hardwood forest watershed ecosystem. Ecosystems, **3**: 159–184. doi:10.1007/s100210000017.

Johnson, C.E., Siccama, T.G., Denny, E.G., Koppers, M.M., and Vogt, D.J. 2014. In situ decomposition of northern hardwood tree boles: decay rates and nutrient dynamics in wood and bark. Can. J. For. Res. **44**: 1515–1524. doi:10.1139/cjfr-2014-0221.

Jonard, M., Fürst, A., Verstraeten, A., Thimonier, A., Timmermann, V., Potočić, N., et al. 2015. Tree mineral nutrition is deteriorating in Europe. Global Change Biol. **21**: 418–430. doi:10.1111/gcb.12657.

Juice, S.M., Fahey, T.J., Siccama, T.G., Driscoll, C.T., Denny, E.G., Eagar, C., et al. 2006. Response of sugar maple to calcium addition to Northern Hardwood Forest. Ecology, **87**: 1267–1280. doi:10.1890/0012-9658(2006)87[1267:ROSMTC]2.0.CO;2.

Keeling, C.D., Piper, S.C., Bacastow, R.B., Wahlen, M., Whorf, T.P., Heimann, M., and Meijer, H.A. 2005. Atmospheric CO_2 and $^{13}CO_2$ exchange with the terrestrial biosphere and oceans from 1978 to 2000: observations and carbon cycle implications. *In* A history of atmospheric CO_2 and its effects on plants, animals, and ecosystems. *Edited by* I.T. Baldwin, M.M. Caldwell, G. Heldmaier, R.B. Jackson, O.L. Lange, and H.A. Mooney, Springer, New York, New York, NY. pp. 83–113. doi:10.1007/0-387-27048-5_5.

Liang, X., Liu, S., Wang, H., and Wang, J. 2018. Variation of carbon and nitrogen stoichiometry along a chronosequence of natural temperate forest in northeastern China. J. Plant Ecol. **11**: 339–350. doi:10.1093/jpe/rtx008.

Lovett, G.M., Weathers, K.C., Arthur, M.A., and Schultz, J.C. 2004. Nitrogen cycling in a northern hardwood forest: do species matter? Biogeochemistry, **67**: 289–308. doi:10.1023/B:BIOG.0000015786.65466.f5.

Lovett, G.M., Arthur, M.A., Weathers, K.C., and Griffin, J.M. 2010. Long-term changes in forest carbon and nitrogen cycling caused by an introduced pest/pathogen complex. Ecosystems, **13**: 1188–1200. doi:10.1007/s10021-010-9381-y.

Luo, Y., Su, B., Currie, W.S., Dukes, J.S., Finzi, A., Hartwig, U., et al. 2004. Progressive nitrogen limitation of ecosystem responses to rising atmospheric carbon dioxide. BioScience, **54**: 731–739. doi:10.1641/0006-3568(2004)054[0731:PNLOER]2.0.CO;2.

Mader, D.L., and Thompson, B.W. 1969. Foliar and soil nutrients in relation to sugar maple decline. Soil Sci. Soc. Am. J. **33**: 794–800. doi:10.2136/sssaj1969.03615995003300050046x.

Mann, T.A., Yanai, R.D., Fahey, T.J., and Reinmann, A.B. 2024. Nitrogen and phosphorus addition affect soil respiration in northern hardwood forests. Ecosystems, **27**: 765–778. doi:10.1007/s10021-024-00912-1.

Mason, R.E., Craine, J.M., Lany, N.K., Jonard, M., Ollinger, S.V., Groffman, P.M., et al. 2022. Evidence, causes, and consequences of declining nitrogen availability in terrestrial ecosystems. Science, **376**: eabh3767. doi:10.1126/science.abh3767.

Mattson, W.J. 1980. Herbivory in relation to plant nitrogen content. Annu. Rev. Ecol. Evol. Syst. **11**: 119–161. doi:10.1146/annurev.es.11.110180.001003.

McNulty, S.G., Boggs, J.L., Aber, J.D., and Rustad, L.E. 2017. Spruce-fir forest changes during a 30-year nitrogen saturation experiment. Sci. Total Environ. **605–606**: 376–390. doi:10.1016/j.scitotenv.2017.06.147.

Norby, R., Warren, J., Iversen, C., Garten, C., Medlyn, B., and McMurtrie, R. 2009. CO_2 enhancement of forest productivity constrained by limited nitrogen availability. Nat. Preced.doi:10.1038/npre.2009.3747.1.

Norby, R.J., Warren, J.M., Iversen, C.M., Medlyn, B.E., and McMurtrie, R.E. 2010. CO_2 enhancement of forest productivity constrained by limited nitrogen availability. Proc. Natl. Acad. Sci. **107**: 19368–19373. doi:10.1073/pnas.1006463107.

Pardo, L.H., Kendall, C., Pett-Ridge, J., and Chang, C.C.Y. 2004. Evaluating the source of streamwater nitrate using δ^{15}N and δ^{18}O in nitrate in two watersheds in New Hampshire, USA. Hydrol. Process. **18**: 2699–2712. doi:10.1002/hyp.5576.

Pardo, L.H., Templer, P.H., Goodale, C.L., Duke, S., Groffman, P.M., Adams, M.B., et al. 2006. Regional assessment of N saturation using foliar and root δ^{15}N. Biogeochemistry, **80**: 143–171. doi:10.1007/s10533-006-9015-9.

Pardo, L.H., Green, M.B., Bailey, S.W., McGuire, K.J., and McDowell, W.H. 2022. Identifying controls on nitrate sources and flowpaths in a forested catchment using a hydropedological framework. J. Geophys. Res. Biogeosci. **127**: e2020JG006140. doi:10.1029/2020JG006140.

Peñuelas, J., Canadell, J.G., and Ogaya, R. 2011. Increased water-use efficiency during the 20th century did not translate into enhanced tree growth. Global Ecol. Biogeogr. **20**: 597–608. doi:10.1111/j.1466-8238.2010.00608.x.

Penuelas, J., Fernández-Martínez, M., Vallicrosa, H., Maspons, J., Zuccarini, P., Carnicer, J., et al. 2020. Increasing atmospheric CO_2 concentrations correlate with declining nutritional status of European forests. Commun. Biol. **3**: 125. doi:10.1038/s42003-020-0839-y.

Perkowski, E.A., Ezekannagha, E., and Smith, N.G. 2025. Nitrogen demand, availability, and acquisition strategy control plant responses to elevated CO_2. J. Exp. Bot. **76**: 2908–2923. doi:10.1093/jxb/eraf118.

Phillips, R.P., Brzostek, E., and Midgley, M.G. 2013. The mycorrhizal-associated nutrient economy: a new framework for predicting carbon–nutrient couplings in temperate forests. New Phytol. **199**: 41–51. doi:10.1111/nph.12221.

Pinhiero, J., and Bates, D., R Core Team. 2025. nlme: linear and nonlinear mixed effects models. R package version 3.1-168. Available from https://CRAN.R-project.org/package=nlme.

Possinger, A.R., Driscoll, C.T., Green, M.B., Fahey, T.J., Johnson, C.E., Koppers, M.M.K., et al. 2025. Increasing soil respiration in a northern hardwood forest indicates symptoms of a changing carbon cycle. Commun. Earth Environ. **6**: 418. doi:10.1038/s43247-025-02405-y.

R Core Team. 2025. R: a language and environment for statistical computing. R Foundation for Statistical Computing, Vienna, Austria. Available from https://www.R-project.org/.

Rastetter, E.B., Ågren, G.I., and Shaver, G.R. 1997. Responses of N-limited ecosystems to increased CO_2: a balanced-nutrition, coupled-element-cycles model. Ecol. Appl. **7**: 444–460. doi:10.1890/1051-0761(1997)007[0444:RONLET]2.0.CO;2.

Reich, P.B., and Oleksyn, J. 2004. Global patterns of plant leaf N and P in relation to temperature and latitude. Proc. Natl. Acad. Sci. **101**: 11001–11006. doi:10.1073/pnas.0403588101.

Reich, P.B., Walters, M.B., and Ellsworth, D.S. 1997. From tropics to tundra: global convergence in plant functioning. Proc. Natl. Acad. Sci. **94**: 13730–13734. doi:10.1073/pnas.94.25.13730.

Reich, P.B., Hungate, B.A., and Luo, Y. 2006. Carbon–nitrogen interactions in terrestrial ecosystems in response to rising atmospheric carbon dioxide. Annu. Rev. Ecol. Evol. Syst. **37**: 611–636. doi:10.1146/annurev.ecolsys.37.091305.110039.

Roco, C.A., Dörsch, P., Booth, J.G., Pepe-Ranney, C., Groffman, P.M., Fahey, T.J., et al. 2019. Using metagenomics to reveal landscape scale patterns of denitrifiers in a montane forest ecosystem. Soil Biol. Biochem. **138**: 107585. doi:10.1016/j.soilbio.2019.107585.

Roth, S., MacDonald, E.P., and Lindroth, R.L. 1997. Atmospheric CO_2 and soil water availability: consequences for tree–insect interactions. Can. J. For. Res. **27**: 1281–1290. doi:10.1139/x97-031.

Sabo, R.D., Elmore, A.J., Nelson, D.M., Clark, C.M., Fisher, T., and Eshleman, K.N. 2020. Positive correlation between wood δ^{15}N and stream nitrate concentrations in two temperate deciduous forests. Environ. Res. Commun. **2**: 025003. doi:10.1088/2515-7620/ab77f8.

Sebestyen, S.D., Ross, D.S., Shanley, J.B., Elliott, E.M., Kendall, C., Campbell, J.L., et al. 2019. Unprocessed atmospheric nitrate in waters of the Northern Forest Region in the U.S. and Canada. Environ. Sci. Technol. **53**: 3620–3633. doi:10.1021/acs.est.9b01276.

Silva, L.C.R., and Anand, M. 2013. Probing for the influence of atmospheric CO_2 and climate change on forest ecosystems across biomes.

Global Ecol. Biogeogr. **22**: 83–92. doi:10.1111/j.1466-8238.2012.00783.x.

Smith, N.G., and Keenan, T.F. 2020. Mechanisms underlying leaf photosynthetic acclimation to warming and elevated CO_2 as inferred from least-cost optimality theory. Global Change Biol. **26**: 5202–5216. doi:10.1111/gcb.15212.

Smith, N.G., Zhu, Q., Keenan, T.F., and Riley, W.J. 2024. Acclimation of photosynthesis to CO_2 increases ecosystem carbon storage due to leaf nitrogen savings. Global Change Biol. **30**: e17558. doi:10.1111/gcb.17558.

St.Clair, S.B., Sharpe, W.E., and Lynch, J.P. 2008. Key interactions between nutrient limitation and climatic factors in temperate forests: a synthesis of the sugar maple literature. Can. J. For. Res. **38**: 401–414. doi:10.1139/X07-161.

Taub, D.R., and Wang, X. 2008. Why are nitrogen concentrations in plant tissues lower under elevated CO_2? A critical examination of the hypotheses. J. Integr. Plant Biol. **50**: 1365–1374. doi:10.1111/j.1744-7909.2008.00754.x.

Templer, P.H., and Dawson, T.E. 2004. Nitrogen uptake by four tree species of the Catskill Mountains, New York: implications for forest N dynamics. Plant Soil, **262–262**: 251–261. doi:10.1023/B:PLSO.0000037047.16616.98.

USDA Forest Service, Northern Research Station. 2024. Hubbard Brook Experimental Forest: Daily Precipitation Rain Gage Measurements, 1956—present ver 22. Environmental Data Initiative. doi:10.6073/pasta/e55baf46bd1c49b38a5806f15fa54801.

USDA Forest Service, Northern Research Station. 2025. Hubbard Brook Experimental Forest: Daily Temperature Record, 1955—present ver 15. Environmental Data Initiative. doi:10.6073/pasta/e698e823085c4edcb7d59b4b7d945b49.

van Doorn, N.S., Battles, J.J., Fahey, T.J., Siccama, T.G., and Schwarz, P.A. 2011. Links between biomass and tree demography in a northern hardwood forest: a decade of stability and change in Hubbard Brook Valley, New Hampshire. Can. J. For. Res. **41**: 1369–1379. doi:10.1139/x11-063.

Wexler, S.K., Goodale, C.L., McGuire, K.J., Bailey, S.W., and Groffman, P.M. 2014. Isotopic signals of summer denitrification in a northern hardwood forested catchment. Proc. Natl. Acad. Sci. **111**: 16413–16418. doi:10.1073/pnas.1404321111.

Whittaker, R.H., Likens, G.E., Bormann, F.H., Easton, J.S., and Siccama, T.G. 1979. The Hubbard Brook Ecosystem Study: forest nutrient cycling and element behavior. Ecology, **60**: 203–220. doi:10.2307/1936481.

Wilson, G., Groffman, P., Martel, L., Green, M.B., Driscoll, C.T., Durán, J., et al. 2025. Changes in soil moisture and its relationships with nitrogen cycle processes in a northern hardwood forest. Can. J. For. Res. **55**: 1–15. doi:10.1139/cjfr-2025-0043.

Wolfe, D.W., Gifford, R.M., Hilbert, D., and Luo, Y. 1998. Integration of photosynthetic acclimation to CO_2 at the whole-plant level. Global Change Biol. **4**: 879–893. doi:10.1046/j.1365-2486.1998.00183.x.

Xu, S., Sardans, J., Zhang, J., and Peñuelas, J. 2020. Variations in foliar carbon:nitrogen and nitrogen:phosphorus ratios under global change: a meta-analysis of experimental field studies. Sci. Rep. **10**: 12156. doi:10.1038/s41598-020-68487-0.

Zukswert, J.M., Vadeboncoeur, M.A., and Yanai, R.D. 2024. Responses of stomatal density and carbon isotope composition of sugar maple and yellow birch foliage to N, P and $CaSiO_3$ fertilization. Tree Physiol. **44**: tpad142. doi:10.1093/treephys/tpad142.

Zukswert, J.M., Vadeboncoeur, M.A., Fahey, T.J., and Yanai, R.D. 2025. Treatment effects of nitrogen and phosphorus addition on foliar traits in six northern hardwood tree species. Oecologia, **207**: 23. doi:10.1007/s00442-025-05664-w.